Journal of Applied Chemistry … JAC http://chemistry.journals.semnan.ac.ir

Selective ultrasound enhanced removal of anionic dyes from binary mixture using multivariate calibration and central composite design modeling by positively charged hyper branched ammonium functionalized magnetic graphene oxide

Zahra Lotfi[a,*], Hassan Zavvar Mousavi[b], S. Maryam Sajjadi[a]
[a]*Department of Chemistry, Faculty of Science, Semnan University, Semnan, Iran.*
[b]*Department of Chemistry,Faculty of Science, University of Guilan, Rasht, Iran.*

Article history:
Received: 21/Oct/2018
Received in revised form: 07/Jan/2019
Accepted: 13/Jan/2019

Abstract

Covalently bonded third generation dendrimer to magnetized graphene oxide nanosheets (DMGO), with high adsorption capacity, were synthesized and efficiently used for simultaneous removal of reactive red 195 (RR) and reactive yellow 145 (RY) dyes. The important parameters like initial concentrations of dyes, sorbent mass and sonication time was optimized using central composite design (CCD) combined with response surface methodology (RSM). Because of the severe overlapping spectra of the dyes, at each removal condition, the dyes concentration were obtained by application partial least squares (PLS) as a powerful multivariate calibration method. The optimized parameters was found to be 12.5 min sonication time, 15 mg of sorbent, RR concentration 20.0 mg L^{-1} and RY concentration 45.0 mg L^{-1}. These optimal condition were achieved the removal percentage of 99.20 and 98.80 % for RR and RY, respectively. In order to evaluate sorption performance, isotherms and kinetics studies were carried out under batch adsorption experiments. The adsorption process follows pseudo-second order reaction kinetic, as well as Langmuir isotherm. The results showed that the sorbent had a maximum adsorption capacity of 53.76 and 73.53 mg g^{-1} corresponds to RR and RY, respectively.

Keywords: Adsorption, Central Composite Design, Multivariate calibration, Isotherm, Kinetic.

1. Introduction

Azo dyes as additive materials have been widely used in many industries such as plastics, leather tanning, textiles, rubber and paper. So the effluent waters released from these industries are usually contaminated with dyes. A significant amount of the total world production of these dyes is estimated to be released into the environment without proper treatment. Because the exposure of drinking water with these substances causes serious harms to humans and aquatic biota, reducing these materials in the effluents is very

important before discharge [1, 2]. Hence, several chemical, physical and biological methods, such as biodegradation [3], membrane separation [4], photo degradation [5], coagulation [6, 7], adsorption [8], electrochemical degradation [9], chemical oxidation [10], and aerobic or anaerobic treatment [11, 12], have been developed to remove dyes and other colored contaminants from wastewaters. Some of these methods are not very efficient. The main reason is that usually dyes have a complex structure that creates them thermal and optical stability and with resistance to many oxidizing agents, chemicals, heat and biodegradation [13]. Among the treatment applied, adsorption is one of the most effective treatment methods. Adsorption is effective, simple and practical methods for removing dye containing waste water because of the availability of a wide variety of sorbents and high efficiency [14]. Many different types of sorbents such as zeolites [15], activated carbon [16], clays [17] and biomass [18] Have been used effectively in removing dyes from waste water.

Techniques that use ultrasound waves coupled with other methods to eliminate toxic pollutions are very effective. Adsorption is a process that couple with ultrasound waves to increase the efficiency [19]. Using ultrasound waves accelerate the chemical process in the adsorption process due to the phenomenon of acoustic cavitation. In the cavitation, growth and collapse of micrometrical bubbles, creates by propagation of a pressure wave through a liquid [20]. In addition, ultrasound wave cavitation effects (collapse, nucleation and growth of tiny gas bubbles) improve the breaking and mass transfer between analytes and sorbent. In this way, analytes mass transfer increase via convection pathway that is due to physical phenomena without any changes in equilibrium characteristics of the adsorption/desorption system [21]. Graphene oxide (GO) with large number of oxidized functional groups and large surface area has strong adsorption abilities [22]. Because of this features, many efforts have been made for functioning the surface of graphene oxide. Polyamidoamine (PAMAM) dendrimers are highly branched polymers with many empty internal cavities, functional end-groups and high local densities of active groups which are able to capture analytes. In dendrimer synthesis, with each generation the number of end groups increased exponentially. Dendrimers are attractive candidates for modification surface of sorbent to obtain more functional group and adsorption capacity. So, dendrimers on the surface of magnetized graphene oxide could be formed and leads to the superiority of good dispersibility, hyper branched Nano architecture and high capacity for analytes capture [23-25]. To the best of our knowledge, we have grafted varying branches of PAMAM dendrimers [up to three generations ($G_{1,2,3}$ PAMAM)] on the surface of magnetic graphene oxide for the first time. Dendrimer grafted MGO were investigated as sorbent for removal of azo dyes. The sorbent has a lot of ammonium groups that is able to form ion–pair by combining with anion dyes. So, electrostatic interaction and hydrogen bonding were considered to be the main mechanism for the dye adsorption.

2. Experimental

2. 1 Materials

The RR and RY dyes were purchased from Daystar Firm (Tehran, Iran).GO was purchased from Nanosany corporation (Mashhad, Iran, http://www.irananotech.com). methyl acrylate (MA, 99%), ethylene diamine (EDA, 99%), (3-Aminopropyl) trimethoxysilane (APTMS) with purity grade of 97%, Iron (II) chloride tetra hydrate (99%) and iron (III) chloride hexa hydrate (98%) were provided by Aldrich (Germany). Stock solutions of dyes were prepared by dissolving the dyes in distilled water and their concentrations were measured by UV–Vis spectrophotometer.

2.2. Instruments

The synthesized sorbent was characterized by field emission scanning electron microscopes (FESEM Sigma, Zeiss, Germany) and transmission electron microscopy (TEM) Zeiss-EM10C - 80 KV. The X-ray diffraction (XRD) of sorbent was measured with a Philips PW1840 X-ray diffractometer (U.S.A) using Co-Ka radiation (λ = 1.78896 A), (40 kV and 25 mA conditions). Fourier transform infrared (FTIR) spectra

were obtained using an S, 8400 Shimadzu at a resolution of 1 cm^{-1}. The absorbance spectra of the dyes solutions were obtained on a Shimadzu UV-1650 PC spectrophotometer (Kyoto, Japan) in the range of 200–800 nm with a pair of 1.0-cm quartz cells. The PLS program of PLS toolbox in Matlab version 8.3 was used for calibration and prediction of analytes.

2.3. Synthesis and characterization of covalently bonded third generation dendrimer to magnetizes graphene oxide nanosheets (DMGO)

Covalently bonded third generation dendrimer to magnetized graphene oxide nanosheets (DMGO) were synthesized according to our previous work [26]. The synthesized sorbent were characterized by transmission electron microscopy (TEM), field emission scanning electron microscopy (FESEM), fourier-transform infrared spectra (FT-IR), X-ray diffraction (XRD) and vibrating sample magnetometry (VSM) [26].

2.4. Measurements of dyes adsorption in their binary solution

According to the experiments designed through CCD method, The removal efficiency of dyes examined in binary solution and batch mode as follows: specified amounts of RR and RY dyes solution (50 mL of at a known concentration of 20 mg L^{-1} and 45 mg L^{-1} for RR and RY) at pH of 4 with a known amount of sorbent (15 mg) and maintained for 12.5 min under ultrasound at room temperature. Finally, sorbent was separated rapidly from the solution by using the Nd-Fe-B magnet. The concentration of dyes was calculated by partial least squares calibration method. The removal percentage of each dye (R %) was calculated by:

$$(R\%) = \frac{C_0 - C_t}{C_0} \quad (1)$$

Where C_0 (mg L^{-1}) and C_t (mg L^{-1}) are the dye concentration at initial and after time t, respectively.

2.5. Central composite design

The central composite design (CCD) based on 30 runs consist of central, cubic and axial points was chosen for modeling and optimization of the ultrasonic assisted simultaneous removal of RR and RY in binary solution. A five-level CCD with four factors (concentration of RR (A), concentration of RY (B), sonication time (C) and sorbent dosage (D)) was used to investigate the effects of factors. The experimental range and levels of independent variables are shown in Table 1. Analysis of variance (ANOVA) as powerful test gives useful knowledge about each parameter contribution in signal as sole and interactive term using Design Expert 7.0.0 software [27].

Table 1 Factors and levels in CCD

Factors	Levels				
	-α	-1	0	+1	+α
Concentration of RR (mg L^{-1})	10	20	30	40	50
Concentration of RY (mg L^{-1})	20	40	60	80	100
Sonication time (min)	5	7.5	10	12.5	15
Sorbent dosage (mg)	2	6.5	11	15.5	20

3. Results and discussion

3.1. pH influence on RR and RY removal

The effect of the solution pH on the adsorption of dyes on DMGO sorbent is shown in Fig. 1. The pH has important effect on properties of sorbent and dyes via affecting the ionization of analytes and surface charge of the sorbent. So, pH values were changed in range of 2-8 and the removal percentages were measured. The variation in the removal percentage with changes in pH values can be explained by the interaction between the analytes and the sorbent. Hydrogen bonding is formed by the interaction between the amine group of the sorbent and the phenolic group of dyes. When pH is too low, the electrostatic repulsion increases due to the protonation of the analytes and the sorbent. Because of the electrostatic interactions between the sorbent and the analytes, we have the highest adsorption percentages at pH 4. But at higher pH values, the number of negative charges increased on the sorbent surface, which results in electrostatic repulsion between the sorbent and the anionic dyes, and consequently the percentage of removal is reduced. In higher pH values

and in the alkaline solution removal percentage is more reduced due to the presence of hydroxide ions and competing between these ions and the anionic dyes for the adsorption sites. The results confirm achievement of high removal percentage of dyes at pH of 4.

Fig. 1. Effect of initial pH value on the adsorption capacity of DMGO. (V=50 mL, m=15 mg, C_{RR}=20 mg L^{-1}, C_{RY}=45 mg L^{-1}, t=12.5 min and T =298 K).

3.2. The simultaneous determination of RR and RY in binary solutions

In order to obtain a suitable calibration models for the determination of dyes in mixture, two data sets for the calibration and the validation of PLS model are required. 15 samples contain of different concentration of RR and RY solutions were synthesized based on orthogonal design and divided into a calibration set of 11 and an independent test set of 4 samples. In PLS algorithm, the success of the analysis is highly depends on the accurate selection of the number of components. In the calibration step, leave one-out -cross validation method was applied in the calibration step to find the number of components which was 2. The statistical results of the model consisted of R^2; the Root of the Mean Squared Error of Calibration samples (RMSEC) and Prediction samples (RMSEP)) values were calculated and reported in Table 2 and 3. These parameters were computed based on the following equations:

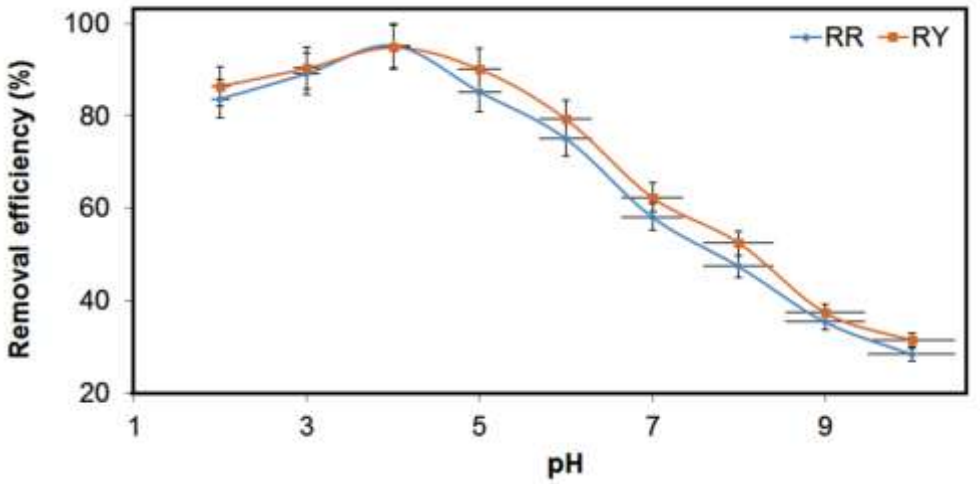

$$R^2 = 1 - \left(\frac{\sum_{i=1}^{I}(c_i - \hat{c}_i)^2}{\sum_{i=1}^{I}(c_i - \bar{c}_i)^2}\right) \quad (2)$$

$$\text{RMSEC} = \sqrt{\frac{\sum_{i=1}^{I}(c_i - \hat{c}_i)^2}{I-1}} \quad (3)$$

Where I; c_i and $\hat{c}_i$ and $\bar{c}_i$ are the total number of samples in the calibration set; the real and predicted concentrations of the given analyte in the i_{th} calibration sample; and the mean of calibration concentrations of analyte, respectively [28-31].

$$\text{RMSEP} = \sqrt{\frac{\sum_{h=1}^{H}(c_h - \hat{c}_h)^2}{H-1}} \quad (4)$$

Where c_h and $\hat{c}_h$ are the real and predicted concentrations of the given analyte in the j_{th} test sample set, respectively. H is the total number of samples in the test set.

The full data set consists of 15 samples is illustrated in Fig 2-a. The results of the calibration and prediction step have been reported in Table 2 and 3, respectively. The obtained statistical parameters of the calibration and prediction steps verified the applicability of PLS model for prediction of the dyes in mixture.

Table 2 Calibration samples and computed statistical parameters of PLS calibration step

Sample number	RR	RY
1	100	80
2	60	80
3	20	80
4	100	40
5	60	40
6	20	40
7	100	15
8	60	15
9	20	15
10	0	50
11	50	0
Statistical parameters		
RMSEC	0.98	1.46
R^2	0.9989	0.9983

Table 3 Test sample and the result of the prediction step of PLS

Sample number	RR	Predicted RR	RY	Predicted RY
1	40	24.98	25	38.55
2	40	61.31	60	39.33
3	80	24.96	25	80.33
4	80	61.16	60	81.47
Statistical parameter				
RMSEP		1.01		1.26

3.3. Experimental design and data analysis

In order to obtain the optimal conditions for the removal with four variables affecting this method, 30 experiments (2^4+ 2 × 4 + 6) were designed. 30 spectra of the residual solution at different experimental conditions were recorded and showed in Fig 2-b.

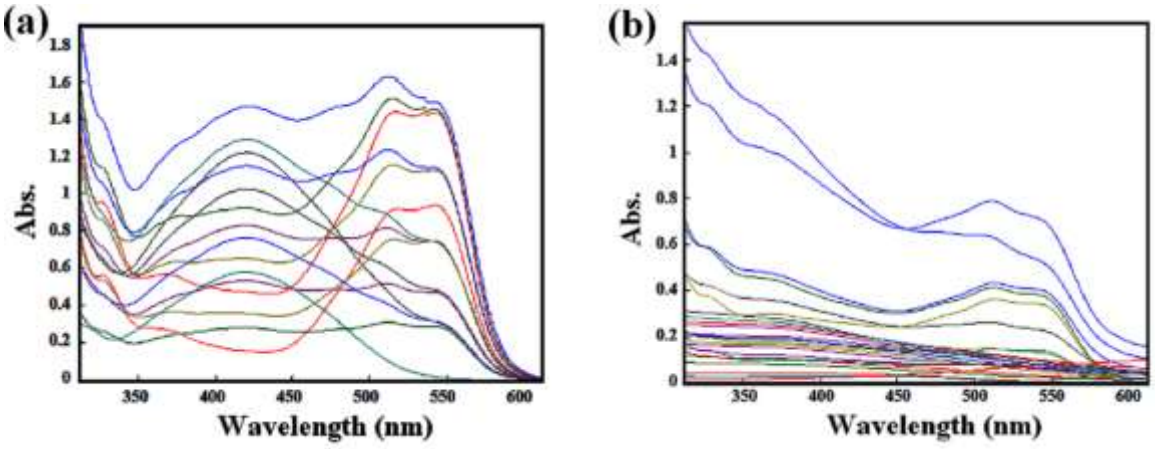

Fig. 2. (a) Spectral profiles of synthesized calibration and prediction samples and (b) Spectral profiles of residual mixture solutions of the dyes at different experimental conditions

C_t of each dye was predicted based on partial lest square and then the recovery were obtained. The main effects of factors were calculated based on analysis of variance (ANOVA) in Table 4. P-values of less than 0.05 in the ANOVA table indicate the statistical significance at 95% confidence level. F-test was used to estimate the statistical significance of all terms in the polynomial equation. According to above definition, the model very low p-value (< 0.0001) and the "Lack of Fit" of 0.9712 and 0.0872 for RR and RY, respectively show the significance of model. Also the values of coefficient R^2, predicted R^2 and the adjusted R^2 show the suitability of model for predicting the real behavior of removal process. Data analysis gave a semi empirical expression with the following equation:

$Y_{RR} = 77.50 - 4.93\text{A} - 5.01\text{B} + 12.12\text{C} + 10.51\text{D} - 1.13\text{AC} - 0.93\text{AD} + 4.43\text{CD} - 1.91A^2 - 2.29B^2 - 6.60C^2 - 6.74D^2$

$Y_{\text{RY}} = 79.10 - 5.01\text{A} - 4.68\text{B} + 11.45\text{C} + 9.93\text{D} + 1.10\text{AB} + 3.68CD - 2.50A^2 - 2.25B^2 - 6.43C^2 - 5.20D^2$

Y_{RR} and Y_{RY} are removal percentages of RR and RY, respectively. A, B, C and D are RR concentration, RY concentration, sonication time and sorbent dosage, respectively. The magnitudes of the coefficients in equations can illustrate the statistical importance of the experimental variables [32]. As can be seen in these equations the factor of sonication time (D) has the most antagonist influence on the removal due to its increasing cause a significant increase in the removal percentage. The obtained data from experimental analysis were evaluated by analysis of variance (ANOVA).

To indicate the significant interactions between the parameters in the removal of the studied dyes, 3D plots for reactive red 195 (RR) were represented in fig 3. The observed curvatures in the RSM plots is due to the quadratic terms [33]. Finally, the optimized parameters were found to be 12.5 min sonication time, 15 mg of sorbent dosage, RR and RY concentrations were 20.0 and 45.0 mg L^{-1}.

3.4. Adsorption isotherm

Adsorption isotherms can describe surface properties and the affinity of sorbents. Thus the experimental data fit to different isothermal models are used to evaluate the adsorption performance of DMGO. In this study, the obtained isotherm data are fitted using the classical Langmuir and Freundlich models, respectively. The Langmuir isotherm assumes the sorbent has a homogeneous adsorption surface, which means all the adsorption sites have equal adsorbed affinities; the model is expressed as:

$$\frac{C_e}{q_e} = \frac{1}{q_{max}k_f} + \frac{C_e}{q_{max}} \quad (5)$$

The q_e(mg g^{-1}) is the adsorption capacity of dyes at equilibrium, q_{max} (mg g^{-1}) is the theoretical maximum adsorption capacity, C_e (mg L^{-1}) represents the concentration of dyes at equilibrium and k_f (L mg^{-1}) is the constant of Langmuir model which related to the energy of binding sites and affinity to adsorption. These constants included q_{max} and k_f can be deduced from the slope and intercept of the linear plot of C_e/q_e *versus* C_e.

Table 4 ANOVA table obtained from CCD analysis for RR and RY

Analytes	Source of variation	Sum of square	Df	P- value	R^2	R^2_{adj}	R^2_{pred}
	Model	9866.05	14	< 0.0001	0.9980	0.9961	0.9941
	Residuals	20.18	15				
RR	LOF	6.68	10	0.9712			
	Pure error	13.50	5				
	Total	9886.23	29				
RY	Model	8580.58	14	< 0.0001	0.9930	0.9864	0.9632
	Residuals	60.78	15				
	LOF	53.28	10	0.0872			
	Pure error	7.50	5				
	Total	8641.36	29				

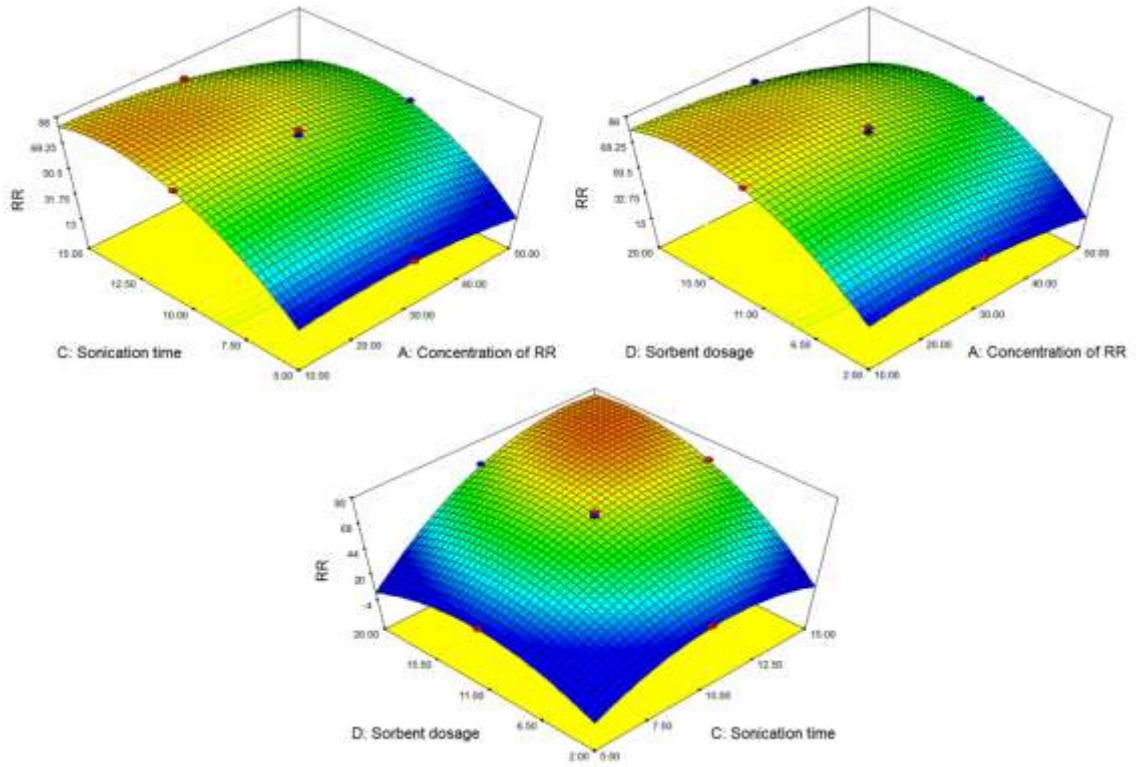

Fig. 3. Three-dimensional RSM plot for removal of RR and RY dyes.

Freundlich isotherm assumes heterogeneous adsorption because of the diversity of the adsorption sites or the diverse nature of the metal ions adsorbed[34]. The Freundlich isotherm model is defined as:

$$log\ q_e = logk_f + \frac{1}{n} logC_e \qquad (6)$$

Where q_e (mg g^{-1}) and C_e (mg L^{-1}) is the equilibrium adsorption capacity and equilibrium concentration of dyes, respectively, n and k_f is the constants of Freundlich isotherm equation, which correspond to adsorption capacity of sorbent and adsorption intensity. Both of them can be calculated from the slope and intercept of the linear plot of log q_e *versus* log C_e.

As shown in Fig. 4-a, b the adsorption capacities arise with the increase of the initial dyes concentration. The fitting results based on the two isotherm models are listed in Table 5. It can be concluded that the adsorption of dyes on sorbent is better estimated by the Langmuir model with the correlation coefficient (R^2) near 1.0, indicating that the adsorption of dyes onto these nano hybrid composite occurs *via* monolayer adsorption. Maximum adsorption capacity calculated from the Langmuir isotherm model is 53.76 and 73.53 mg g^{-1} for RR and RY, respectively. A comparison was made between maximum adsorption capacity values of RR and RY dyes by some adsorbents and results are shown in table 6.

Table 5 Constants and correlation coefficients for isotherm models

Analyte	Langmuir			Freundlich		
	q_{max}	K_l	R^2	n	K_f	R^2
RR	53.76	0.099	0.997	3.49	3.33	0.977
RY	73.53	0.810	0.998	17.48	5.79	0.939

Table 6 Comparison maximum adsorption capacity of various reactive dyes by some adsorbents

Adsorbent	Adsorbate	Adsorption capacity (mg/g)	Refs.
Carbon nanotubes	RR	29.94	[35]
Calcined alunite	RY	57.20	[36]
Wood-shaving bottom ash	RR	24.3	[37]
Waste metal hydroxide	RR	48.3	[38]
Fly ash	RR	47.26	[39]
	RY	37.26	
DMGO	RY	73.53	This work
	RR	53.76	

3.5. Adsorption kinetics

It's known that the adsorption process of analytes depends on a mix of multiple mechanisms such as mass transfer, diffusion control, chemical reactions and particle diffusion. In order to understand the dyes adsorption kinetic on DMGO, the experimental data collected at the dyes concentration of (RR 20 mg L^{-1} and RY 45 mg L^{-1}) in pH 4.0 and different times were fitted with the Lagergren pseudo-first-order and pseudo-second-order kinetic models[40]. The pseudo-first-order and pseudo-second-order kinetic models can be described as:

$$\ln(q_e - q_t) = \ln(q_e) - k_1 t \quad (7)$$

$$\frac{t}{q_t} = \frac{1}{k_2 q_e^2} + \frac{1}{q_e} t \quad (8)$$

Where q_e (mg g^{-1}) and q_t (mg g^{-1}) are the amounts of the dyes adsorbed at equilibrium and at time t (min), respectively; k_1 (min^{-1}) and k_2 (g $(mg.min)^{-1}$) are the kinetic rate constants for the pseudo-first-order and the pseudo-second-order models, respectively. The validities of these two kinetic models are examined and depicted in Fig. 4-c, and the values of the parameters and the correlation coefficients obtained from these two kinetic models are all listed in Table 7. The results suggest that the dyes adsorption process on DMGO follow the pseudo-second-order kinetic model.

3.6. Effect of inorganic anion competition

Cl^-, NO_3^-, SO_4^{2-} and PO_4^{3-} are the common anions that usually exist in natural water and wastewater, and the same negative-charge and high level concentration might lead to the competition adsorption between common anions with dyes. Thus, it is essential to study the adsorption efficiency of DMGO sorbent toward dyes removal with the coexistence of common anions. In this study, we were spiked Cl^-, NO_3^-, SO_4^{2-} and PO_4^{3-} with different concentration ratio ranging from 1:2 (10 mg L^{-1} anions and 20 mg L^{-1} RR) to 5:1 (100 mg L^{-1} anions and 20 mg L^{-1} RR) into reactive red 195 solution . The dyes removal efficiency under different concentration ratio is shown in Fig. 5. The results indicate with increasing molar ratios of chloride and nitrate ions, removal efficiency decreased slightly. So, it is obvious that the effect of chloride and nitrate ions is negligible or very small. Because dendrimer on the surface of sorbent is a highly branched polymers with many empty internal cavities, functional end-groups and high local densities of active groups which are able to capture analytes. While on the contrary, increase in the concentration of sulphate and phosphate ions causes higher reduction on the adsorption of the dyes. This observed inhibition by the sulphate and phosphate anions can be interpreted by the competitive adsorption of anions with RR on the surface of DMGO, since at pH=4, adsorption is dominated by electrostatic attraction, and consequently, the binding of multivalent anions with the sorbent is strong.

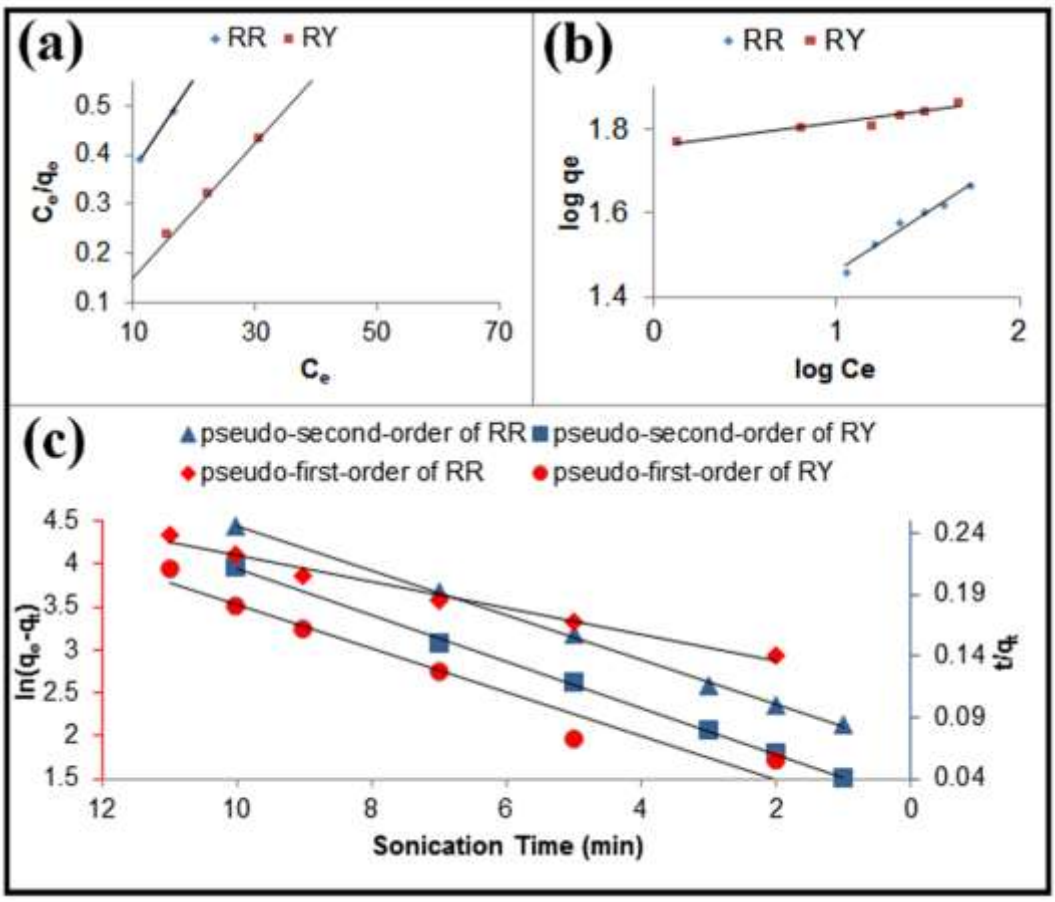

Fig. 4. Adsorption isotherm of dyes on DMGO and fitting results for the (a) Langmuir and (b) Freundlich isotherm models. (c) Adsorption kinetic of dyes on DMGO and fitting results for the pseudo-first-order and pseudo-second-order kinetic models.

Table 7 Constants and correlation coefficients for the kinetic models

Analyte	pseudo first-order			pseudo second-order		
	q_e	K_1	R^2	q_e	K_2	R^2
RR	81.54	0.1529	0.9869	54.94	0.0051	0.9991
RY	56.52	0.2538	0.9587	53.19	0.0155	0.9991

3.7. Selective adsorption of anionic dyes

The ability of a sorbent to selectively adsorb analytes is a very important factor and should be investigated. For this purpose, experiments were carried out in a mixture of anionic dye (reactive red 195, 20 mg L^{-1}) and cationic dye (Brilliant green, 20 mg L^{-1}). The RR removal efficiency with DMGO sorbent in the anionic and cationic mixture solution was more than 95%. While the removal efficiency for cationic dye was small and about 10%. The experimental results indicate that the removal of anionic dye was performed completely while that for the cationic dye is not impressive. The experimental observation indicates that an electrostatic interaction between anionic dye and NH_2 groups is primarily responsible for the selective adsorption of anionic dyes from their mixture. This further supports the possibility of using DMGO as a sorbent for selective removal of anionic dyes.

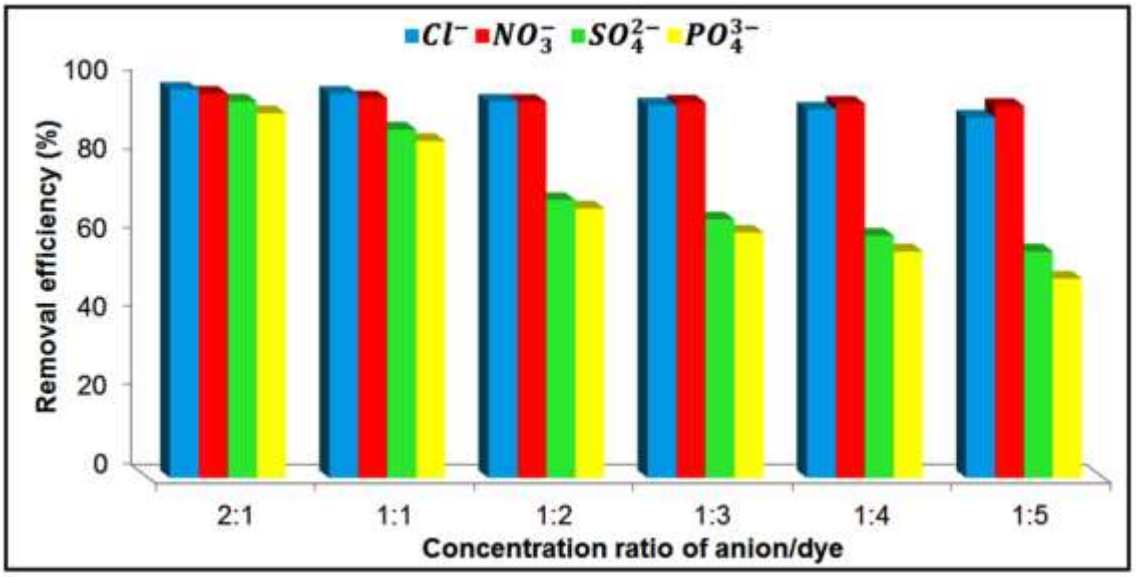

Fig. 5. Effect of coexisting anions on adsorption capacity of RR onto DMGO sorbent under different concentration ratio.

3.8. Desorption and reusability experiments

The ability to reuse a sorbent is very essential in removal application. A good sorbent should possess high adsorption capability as well as good desorption property. So, the ability to reuse is an important factor in evaluating the acceptable sorbent. For regeneration, the recycled sorbents were first washed with sodium hydroxide (0.1 M) and then hydrochloric acid (0.1 M), and then were used for the next adsorption process. Note that the whole regeneration process is only several minutes. The regeneration cycles were repeated more than 6 times. The results show that DMGO could be recycled and reused for at least 6 times with a stable adsorption of more than 90%.

4. Conclusion

In conclusion, due to the high cationic charge density of DMGO in pH=4, the DMGO sorbent can fast and selectively adsorb anionic dyes from mixed dyes via electrostatic interaction, and the separation efficiency can up to 98%. Notably, the sorbents can maintain their high efficiency (>90%) even after 6 cycles, and the regeneration process can be accomplished only within several minutes, showing desirable and fast regeneration ability. The adsorption process for anionic dyes follows pseudo-second order reaction kinetics, as well as Langmuir isotherm, indicating that anionic dyes are monolayer adsorbed on the sorbent by electrostatic interaction. DMGO sorbent with selective adsorption ability and high recyclability exhibits favorable and unique flexibility and potential in dyes wastewater treatment.

Acknowledgments

We are grateful to Semnan University for its financial support.

References

[1] M. Bhowmik, K. Deb, A. Debnath, B. Saha, *Applied Organometallic Chemistry*, (2017).

[2] N.H. Singh, K. Kezo, A. Debnath, B. Saha, *Applied Organometallic Chemistry*, (2017).

[3] S.K. Garg, M. Tripathi, *Environmental monitoring and assessment*, **185** (2013) 8909.

[4] X. Ma, P. Chen, M. Zhou, Z. Zhong, F. Zhang, W. Xing, *Industrial & Engineering Chemistry Research*, (2017).

[5] P. Mohammadi, H. Sheibani, *Applied Organometallic Chemistry*, (2018).

[6] N.M. Mahmoodi, *Environmental monitoring and assessment*, **186** (2014) 5595.

[7] R. Li, B. Gao, K. Guo, Q. Yue, H. Zheng, Y. Wang, *Bioresource Technology*, (2017).

[8] S. Porhemmat, A. Rezvani, M. Ghaedi, A. Asfaram, A. Goudarzi, *Applied Organometallic Chemistry*, **31** (2017).

[9] B. Rezaei, H. Khosropour, A. Ensafi, A, *Analytical Methods*, **9** (2017) 267.

[10] I. Arslan, I.A. Balcioğlu, D.W. Bahnemann, *Dyes and pigments*, **47** (2000) 207.

[11] B. Liang, Q. Yao, H. Cheng, S. Gao, F. Kong, D. Cui, Y. Guo, N. Ren, A. Wang, *Environmental Science and Pollution Research*, **19** (2012) 1385.

[12] B. Frindt, J. Mattusch, T. Reemtsma, A.G. Griesbeck, A. Rehorek, *Environmental Science and Pollution Research*, **24** (2017) 10929.

[13] J. Pooralhossini, M.A. Zanjanchi, M. Ghaedi, A. Asfaram, M.H.A. Azqhandi, *Applied Organometallic Chemistry*, (2018).

[14] S. Jalali, M.R. Rahimi, M. Ghaedi, A. Asfaram, A. Goudarzi, *Applied Organometallic Chemistry*, **32** (2018).

[15] E. Rosales, M. Pazos, M. Sanromán, T. Tavares, *Desalination*, **284** (2012) 150.

[16] H. Jamshidi, M. Ghaedi, M.M. Sabzehmeidani, A.R. Bagheri, *Applied Organometallic Chemistry*, (2017).

[17] E. Errais, J. Duplay, F. Darragi, I. M'Rabet, A. Aubert, F. Huber, G. Morvan, *Desalination*, **275** (2011) 74.

[18] P. Pengthamkeerati, T. Satapanajaru, N. Chatsatapattayakul, P. Chairattanamanokorn, N. Sananwai, *Desalination*, **261** (2010) 34.

[19] Z. Lotfi, H.Z. Mousavi, S.M. Sajjadi, *Rsc Advances*, **6** (2016) 90360.

[20] Z. Lotfi, H.Z. Mousavi, S.M. Sajjadi, *Microchimica Acta*, **184** (2017) 1427.

[21] M. Roosta, M. Ghaedi, N. Shokri, A. Daneshfar, R. Sahraei, A. Asghari, *Spectrochimica Acta Part A: Molecular and Biomolecular Spectroscopy*, **118** (2014) 55.

[22] Z. Lotfi, H. Zavvar Mousavi, S.M. Sajjadi, *Applied Organometallic Chemistry*, **32** (2018) 4162.

[23] Y. Xu, Z. Zhang, J. Zheng, Q. Du, Y. Li, *Applied Organometallic Chemistry*, **27** (2013) 13.

[24] S.J. Tabatabaei Rezaei, A. Mashhadi Malekzadeh, S. Poulaei, A. Ramazani, H. Khorramabadi, *Applied Organometallic Chemistry*, **32** (2018).

[25] Z. Lotfi, H.Z. Mousavi, S.M. Sajjadi, *Analytical Methods*, **9** (2017) 4504.

[26] Z. Lotfi, H.Z. Mousavi, S.M. Sajjadi, *Microchimica Acta*, (2017) 1.

[27] J. Zolgharnein, A. Shahmoradi, J.B. Ghasemi, *Journal of Chemometrics*, **27** (2013) 12.

[28] C.D. Brown, P.D. Wentzell, *Journal of chemometrics*, **13** (1999) 133.

[29] H.L. Wu, Y. Li, R.Q. Yu, *Journal of Chemometrics*, **28** (2014) 476.

[30] J.B. Cooper, C.M. Larkin, M.F. Abdelkader, *Journal of Chemometrics*, **25** (2011) 496.

[31] F. Stout, M.R. Baines, J.H. Kalivas, *Journal of chemometrics*, **20** (2006) 464.

[32] M. Razi-Asrami, J.B. Ghasemi, N. Amiri, S.J. Sadeghi, *Environmental Monitoring and Assessment*, **189** (2017) 196.

[33] A. Rouhollahi, M. Kouchaki, S. Seidi, *RSC Advances*, **6** (2016) 12943.

[34] Y. Zou, X. Wang, Y. Ai, Y. Liu, Y. Ji, H. Wang, T. Hayat, A. Alsaedi, W. Hu, X. Wang, *Journal of Materials Chemistry A*, **4** (2016) 14170.

[35] C.-H. Wu, *Journal of hazardous materials*, **144** (2007) 93.

[36] M. Özacar, I.A. Şengil, *Journal of hazardous materials*, **98** (2003) 211.

[37] P. Leechart, W. Nakbanpote, P. Thiravetyan, *Journal of environmental management*, **90** (2009) 912.

[38] S. Netpradit, P. Thiravetyan, S. Towprayoon, *Water research*, **38** (2004) 71.

[39] N. Dizge, C. Aydiner, E. Demirbas, M. Kobya, S. Kara, *Journal of Hazardous Materials*, **150** (2008) 737.

[40] B. Xiang, W. Fan, X. Yi, Z. Wang, F. Gao, Y. Li, H. Gu, *Carbohydrate polymers*, **136** (2016) 30.